CHAPTER 4

Synthesis of α-Fe_2O_3 nanopowder by using EDTA based precursor method

4.1 Experimental Procedure for Chemical Synthesis:

The starting chemicals used were ferric nitrate nonahydrate (99.9%, Merck, India), ethylenediamine tetracetic acid (EDTA, 99.9%, Merck, India) without further purification.

EDTA was dissolved in water by adding to it, a 50 percent ammonia solution drop wise, till all EDTA was exactly dissolved. Aqueous solutions of EDTA (pH ~ 5) and ferric nitrate were then mixed vigorously in a molar ratio of 1:1 by using a magnetic stirrer. A dark brown colored fluffy precursor was formed when this mixture was dried on a hot plate at ~125^0C.

Iron oxide powder was prepared by grinding this dark brown precursor powder followed by calcination in air for two and a half hours at different temperatures ranging from 250 - 450^0C [123, 124, 130-132]. In order to avoid contamination of the precursor by carbon, a few drops of saturated ammonium nitrate solution was added to the precursor powders at the time of calcination.

4.2 Results and Discussion:

4.2.1 Thermal Analysis:

TG-DTG and DSC analyses were performed to investigate the decomposition behavior of the precursor powders due to heat treatment in air and thermograms are shown in Fig 4.1.

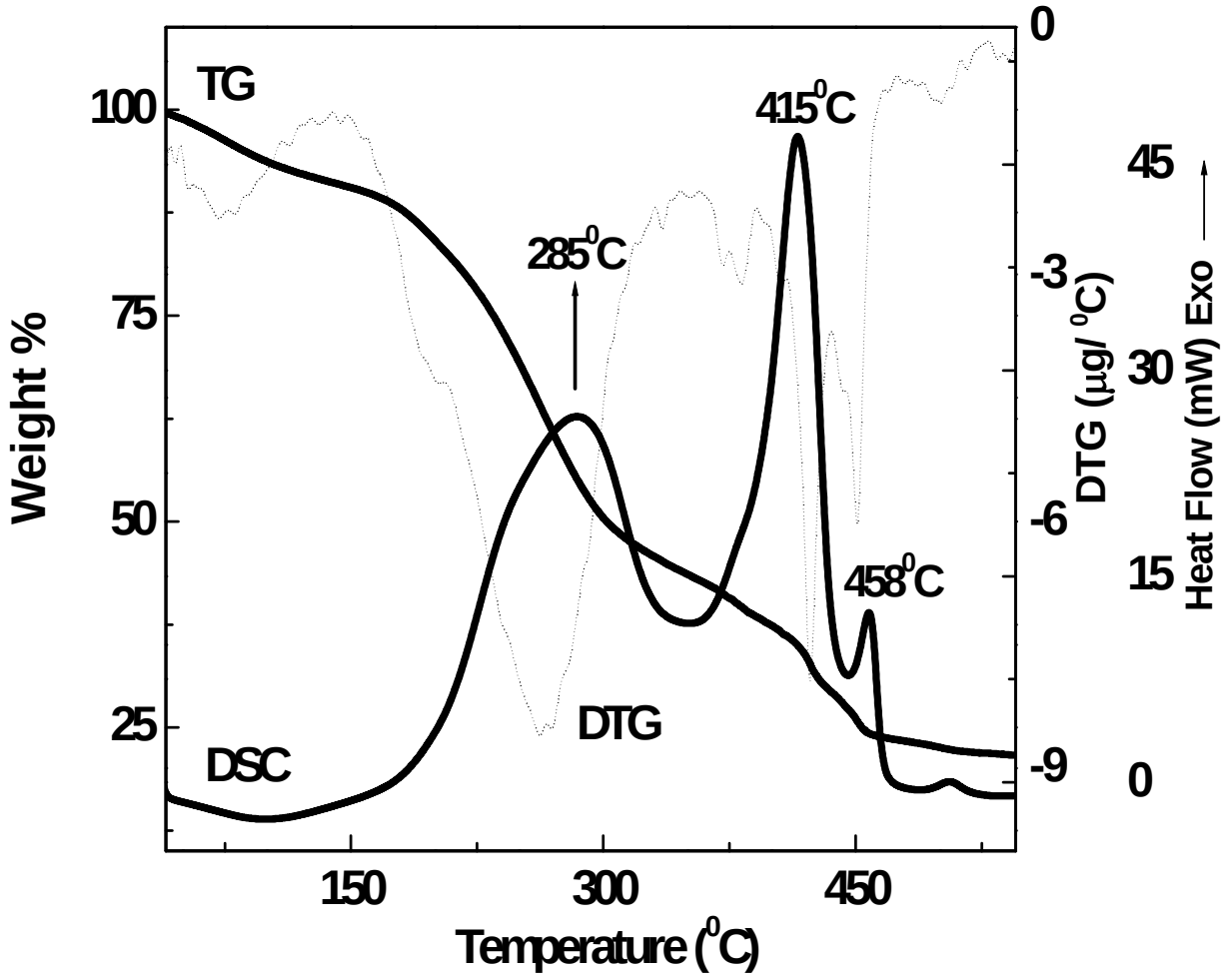

Fig 4.1 TG-DTG and DSC thermograms of the precursor in air.

The main features of the thermograms are described below:

(i) In TG thermogram, a total weight loss of ~ 76% was observed in the temperature range of 40-460^{0}C.

(ii) Minor weight loss of ~8% was observed in the temperature range of 40-140^{0}C that was due to loss of moisture from the sample. This loss was clearly observed in DTG thermogram as an endothermic peak at 74^{0}C

(ii) Thermal decomposition of precursor occurred in two major weight loss steps of ~48% and ~ 20% in the temperature region of 140 - 350^{0}C and 355 - 460^{0}C respectively. This decomposition was due to the oxidative decomposition of precursor, accompanied by the evolution of CO_2 and NO_x gases. It was reflected in DSC thermogram as exothermic peaks at 285, 415, and 458^{0}C.

(iii) Heating the sample beyond 460^{0}C showed neither a weight loss in TGA nor formation of any new peak in DSC thermogram, confirming the completion of decomposition of the precursor to iron oxide at ~460^{0}C [123, 124, 130-132].

4.2.2 X-Ray Analysis:

Room temperature XRD spectra of precursor and precursor powder at different calcination temperatures are shown in Fig. 4.2.

The notable features of the XRD spectra of precursor and calcined powders are as follows:

(i) Formation of pure α-Fe_2O_3 phase was observed in the precursor, which did not undergo any calcination. To the best of our knowledge, precursor containing α-Fe_2O_3 phase has not yet been reported for any other precursor based method.

(ii) Complete formation of single phase α-Fe_2O_3 occurred when precursor was calcined at 450^{0}C for two and a half hours in air [123, 124, 130-132]. Appearance of diffraction peaks at 2θ = 24.4^0, 33.3^0, 35.8^0, 41.0^0, 49.5^0, 54.3^0, 57.7^0, 62.6^0, and 64.2^0 were in good agreement with the corresponding (012), (104), (110), (113), (024), (116), (018), (214) and (300) diffraction planes of α-Fe_2O_3 respectively (JCPDS 80-2377).

(iii) Slow scan of the two main intensity peaks was performed and crystallite size of powders calcined at different temperatures was calculated using Scherrer's equation [125]. They lie in the range of 30-35 nm depending upon the calcination temperature.

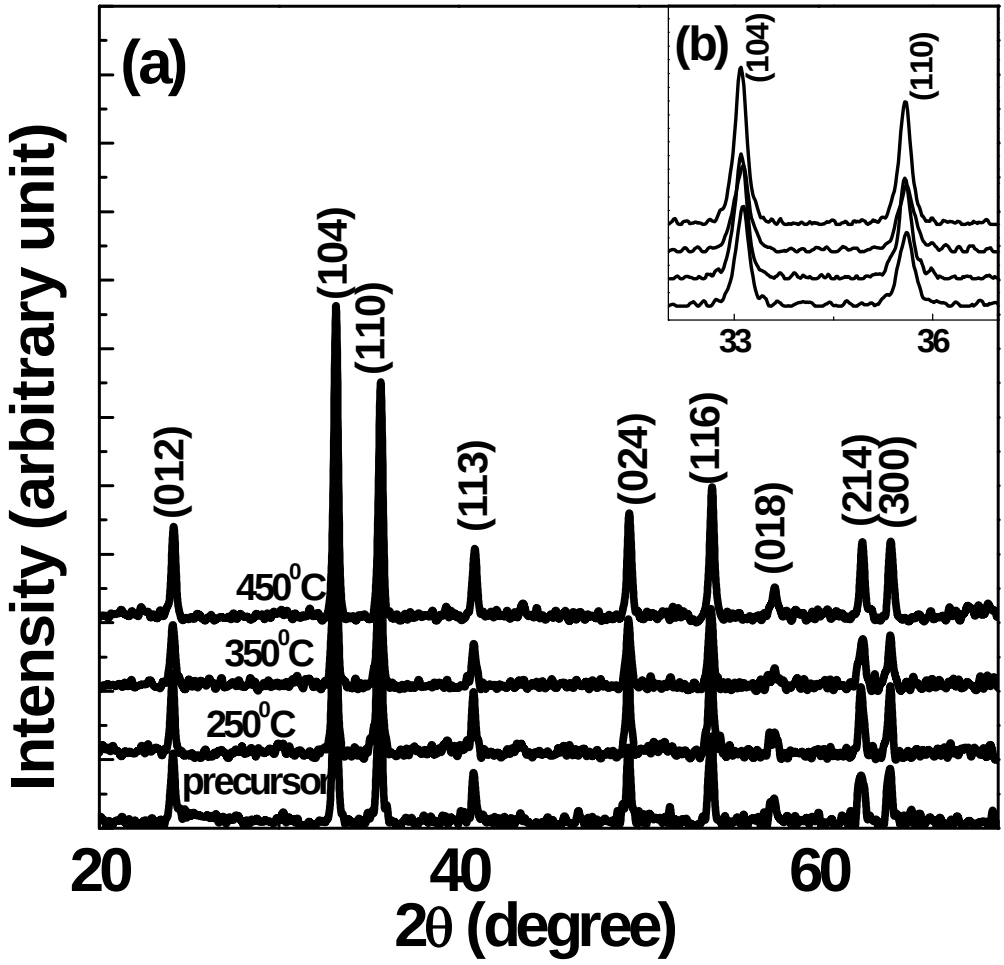

`

Fig 4.2 (a) X-ray diffraction spectra of precursor powder at different calcination temperatures (b) slow scan of the (104) and (110) diffraction planes.

4.2.3 TEM Analysis:

The TEM micrograph of the precursor powder calcined at 450^0C is shown in Fig. 4.3. It clearly indicated that average particle size of the calcined powder is ~35 nm and it matched well with that calculated by using XRD analysis. The particles were mostly elongated in shape and formed loose aggregates.

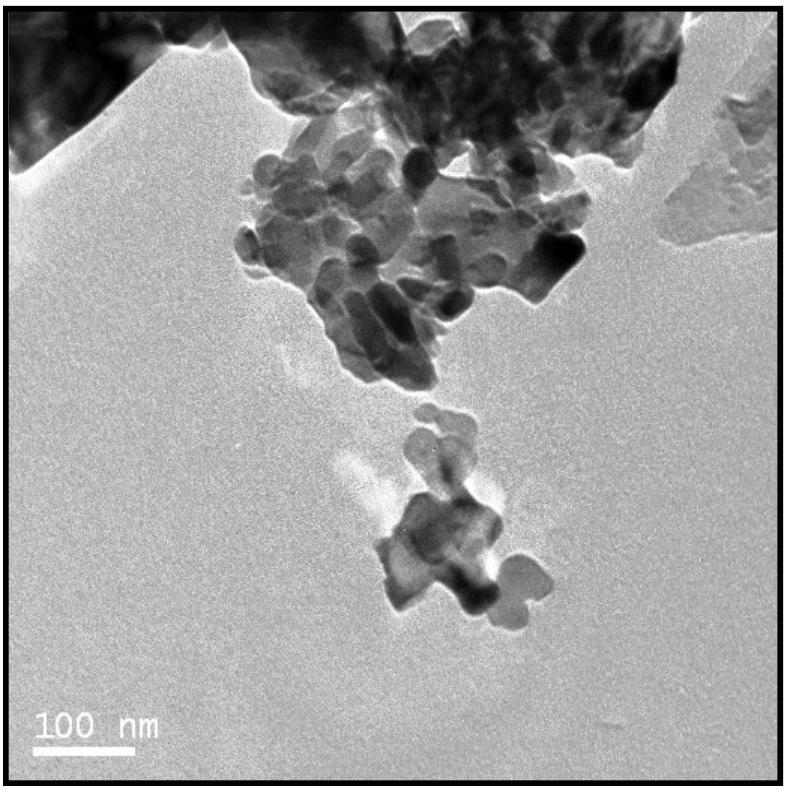

Fig. 4.3 TEM micrograph of α-Fe_2O_3 powder calcined at 450^0C.

4.2.4 SEM Analysis:

SEM was used to study the surface morphology of the unsintered nanopowder as well as of the sample sintered at 1100^0C for 2 hours. The micrographs are shown in Fig. 4.4(a) and (b).

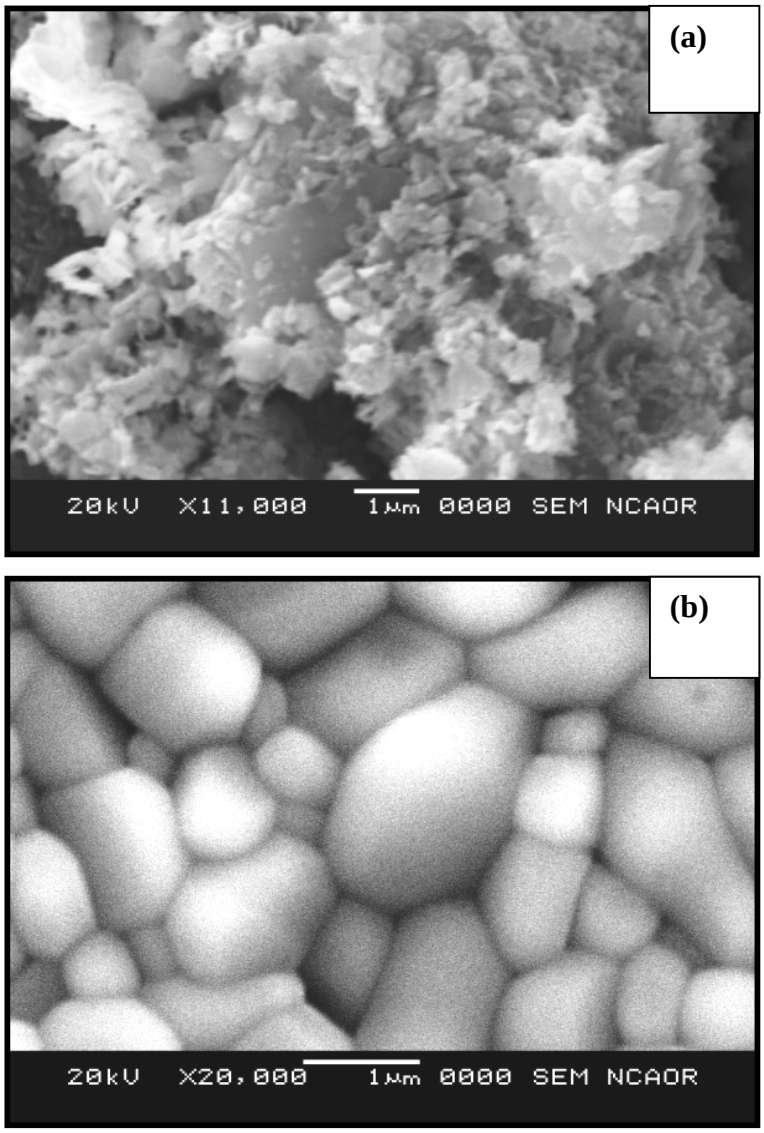

Fig. 4.4 SEM micrographs of α-Fe_2O_3 powder (a) calcined at 450^0C and (b) sintered at 1100^0C.

The micrographs exhibited the following features:

(i) The microstructure of the as-synthesized nanopowder (4.3(a)) constituted of loosely bound nanoparticles with high intergranular porosity.

(ii) Sintering the nanoparticles at high temperature resulted in a uniform microstructure constituting of micron-sized grains. Coarsening of grains at elevated temperature was observed due to fusion of the nanosize particles.

(iii) The particles in both cases were found to be elongated and the shape of particles was in *sync* with the hexagonal corundum structure of α-Fe_2O_3 [1].

4.2.5 DC resistivity measurement:

The variation of resistivity with change in temperature was studied for two cases (i) unsintered pellet and (ii) pellet sintered at 1100^0C and these are shown in Fig. 4.5. Room temperature recorded was 28^0C. The green density and sintered density of the pellets was calculated by using the dimensions of the pellets.

Case (i) unsintered pellet

As seen in SEM micrograph (Fig. 4.4(a)), the powder was nanosized and loosely agglomerated, and therefore, moisture was trapped on the surface and within the pores of the sample. This was responsible for the initial decrease in resistivity from room temperature to 55^0C. The adsorption of moisture (humidity recorded in our lab was 91%) was pronounced as a dip [124, 130-132]. A maximum in resistivity was recorded at ~100^0C that signified complete loss of entrapped moisture from the sample [12, 13, 123, 126, 131]. Beyond ~100^0C, when all moisture was eliminated, the curves exhibit the typical NTCR (negative temperature coefficient of resistance) behavior of bulk hematite [127].

Case (ii) pellet sintered at 1100^0C

The sintered sample attained a densification of ~ 4.2 g/cm^3 which was lower than that obtained in case of PVA precursor based method and comparable to that of Oxalate precursor based method. The resistivity behavior for the sintered sample was affected by the presence of humidity.

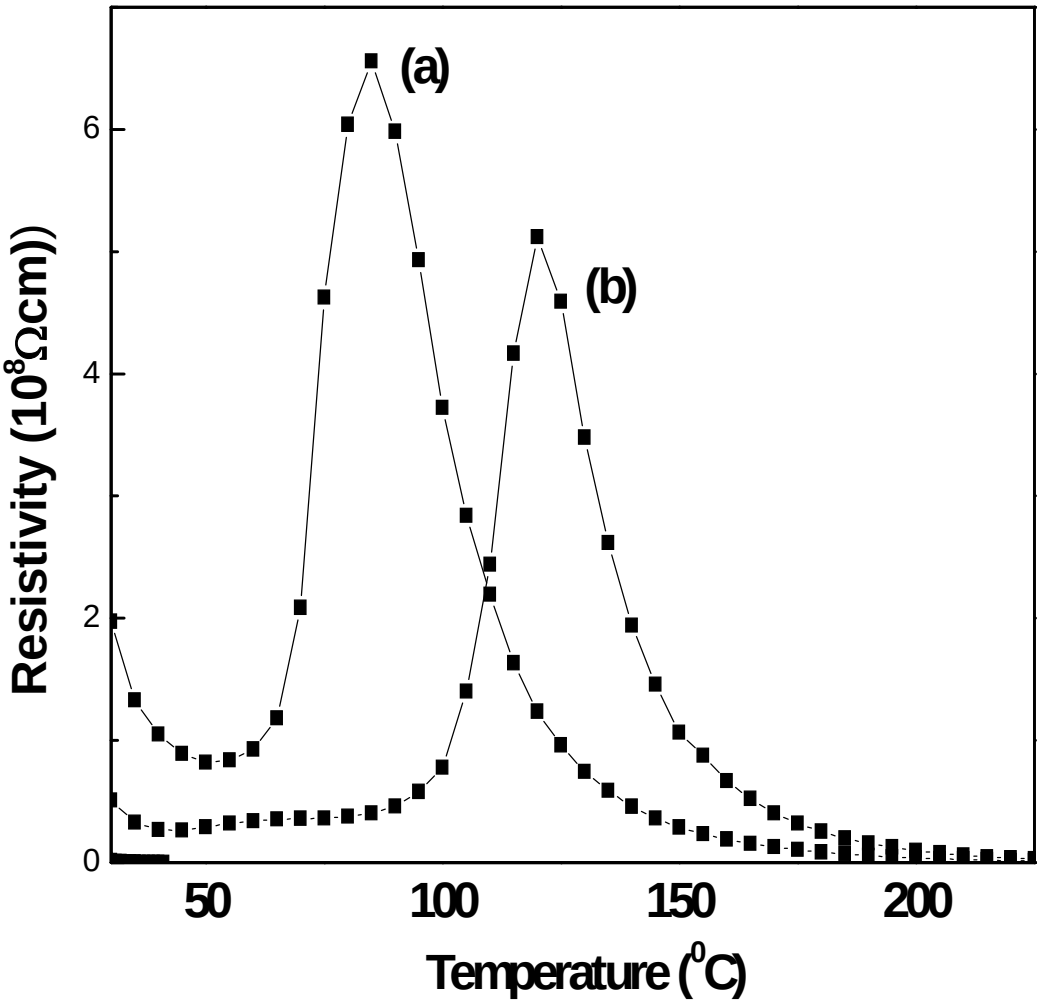

Fig. 4.5 Variation of DC resistivity of synthesized α-Fe_2O_3 with change in temperature for (a) unsintered sample (b) sample sintered at 1100^0C.

However, the effect of moisture in the resistivity behavior was less pronounced as compared to that of the as-synthesized nanopowder. The initial decrease in resistivity observed from room temperature till ~55^0C (Fig. 4.5(a)) corresponding to the adsorption of moisture was absent in case of sintered sample (Fig. 4.5(b)). Microstructure observed in SEM micrograph (Fig. 4.4(b)) of the sintered sample supported its resistivity behavior with respect to temperature.

Discussion:

TGA-DSC, XRD and TEM analysis of the synthesized precursors and calcined powders confirmed that oxidative decomposition of precursor leads to the formation of single phase α-Fe_2O_3 nanopowders. In this chemical method, a homogeneous aqueous solution of iron (III) nitrate and EDTA, on complete dehydration, produces a fluffy, voluminous, carbon-rich mass known as "precursor" powder. The chelating agent, EDTA, plays a critical role. It not only prevents the segregation or intermittent precipitation of metal ions from solution during evaporation but also acts as the fuel to provide the heat through combustion for the formation of the iron oxide phase. During thermal decomposition of precursor, nascent metal oxides forms, which are small atomic clusters with proper chemical homogeneity and these nascent metal oxides finally produce α-Fe_2O_3 nanopowders. The heat provided by the carbonaceous mass of the precursor during thermal decomposition helps in lowering down of the external temperature required for the formation of the phase. Moreover, the evolution of various gases (such as water vapour, CO, CO_2, NO_x) during decomposition of the precursor helps it to disintegrate and dissipate the heat of decomposition. This inhibited the sintering of fine particles during the process to produce nanosized iron oxide [57, 123, 130].

SEM micrographs and DC resistivity measurements indicated that the resistivity behavior with respect to temperature of the synthesized nanopowders as well as sintered sample (although less pronounced) was affected by the presence of moisture in the air due to high porosity in the samples. This indicates a correlation between the microstructure and DC resistivity measurement for the powder synthesized by EDTA precursor based method [123, 124, 131].

4.3 Summary of Results:

1. α-Fe_2O_3 nanopowder was successfully synthesized by using EDTA precursor based synthesis route.
2. Thermal decomposition of the precursor was complete at ~460^{0}C.
3. Single phase α-Fe_2O_3 was formed at a calcination temperature of 450^{0}C for two and a half hours in air.
4. Average particle size of the nanopowder was ~35 nm.
5. Surface morphology studies revealed that the particles were elongated in shape for nanopowders as well as sintered samples.
6. Room temperature resistivity of as-synthesized nanopowder was ~10^8 Ω cm.